

Numerical Modelling of Non-Newtonian Blood Flow Through Multiple Stenosed Artery

Joydeb Sarkar Shuvo, Ahmed Abrar Shayor*, Abdullah Al-Faruk

¹ Department of Mechanical Engineering, Khulna University of Engineering & Technology, Khulna-9203, BANGLADESH

² Department of Mechanical Engineering, Khulna University of Engineering & Technology, Khulna-9203, BANGLADESH

³ Department of Mechanical Engineering, Khulna University of Engineering & Technology, Khulna-9203, BANGLADESH

ABSTRACT

In this numerical simulation, the main aim is to identify the flow characteristics of blood flow through multiple stenosed arteries. Various numerical simulations have been performed in the past, with laminar flow and the artery was assumed to have a rigid wall and blood as a non-Newtonian fluid. A viscous model, namely the Carreau model, was used for the variable viscosity of blood. In multiple stenosis assumptions, the stenosis area is considered as 86% constriction & 75% constriction in the artery vessel. However, stenosis can disrupt the blood flow, resulting in a transition from laminar to turbulent flow when the constriction is sufficiently high. The results were analyzed by using the $k-\omega$ turbulence model in this case. By increasing the spacing distance blood flow characteristics were investigated here. The primarily developed laminar flow behaves more unstable in the stenosed region. Shear stress increases & decreases more quickly while a transitional point in the blood flow as expected at the stenosis region. Thus, resulting in the transition from laminar to turbulent velocity range while flowing from the inlet to the outlet of the modelled section of the artery. A severe level of pressure drop is found at 86% stenosis region compared to 75% stenosis region as was expected. In case of multiple stenosis regions, pressure is dropped in multiple regions which can cause the instability of blood pressure & hamper the human natural blood flow rate and in turn reduce oxygen supply and such blood carried constituents. So multiple stenoses have higher impacts than single stenosis. Flow characteristics for single stenosis differ from multiple stenoses. Multiple stenoses have a higher impact on heart problems than single stenosis. Spacing distances between the multiple stenosis regions have also a great impact. Lower spacing distance has a higher level of discomfort scenario. In the pre-stenotic region fluid flow remains laminar. On the other hand, in the stenotic region flow characteristics remain transitional & in the post stenotic region, the fluid flow behaves as laminar flow again. There were the key findings that would help in medical diagnosis and disease study by providing more knowledge into thrombosis effects and detection.

Keywords: CFD, Blood Flow, Multiple Stenosis, Non-Newtonian, Artery

1. Introduction

Plaques form when cholesterol develops in an arterial wall and connective tissue proliferates, restricting the blood flow in the heart and brain. The term for this condition is called stenosis. This flow pattern may stimulate continued and possibly more aggravated progression of the stenosis once the local constriction or stenosis becomes severe enough to produce a zone of flow separation. Moderate and severe stenoses might cause a flow disturbance downstream of the stenosis. Depending on the rate of flow through the stenosis and the geometry of stenosis, these perturbed flows may remain laminar or may become turbulent. Because turbulence indicates an aberrant flow condition in the circulation, the emergence of turbulent flow has significant therapeutic implications. Cardiovascular disease (CVD) has been one of the leading causes of death in recent years, accounting for roughly 17.9 million deaths worldwide in 2016, which is 31% of total deaths. Among these 85 per cent of these deaths are due to heart attacks and strokes [1].

Besides, knowing the blood flow characteristics like velocity, flow rate and pressure drop can also help biomedical engineers create biomedical types of equipment for treatment (surgical) modalities.

Example: Single & multiple stenoses in human artery which cause severe level of heart problems & diseases.

Several studies were carried out to observe the effect of stenosis when blood flows through a constricted artery,

considering blood as Newtonian. But the supposition of According to Rabby et al. Newtonian behavior of blood is suitable for flow in big arteries and under conditions of high Reynolds number and high shear rate. There are times (like diastole and the beginning of systole) when pulsatile blood flow has a low Reynolds number. According to Rabby et al., non-Newtonian blood flow behavior is acceptable when shear rate is minimal (less than 100 s^{-1}) [2]. Tu et al. (1992) performed a numerical analysis using finite element method considering steady and pulsatile blood flow for various levels of area reduction and Reynolds numbers in the artery with an inflexible wall. They considered 2D blood flow and there is no standard turbulent model like $k-\epsilon$ or $k-\omega$ [3].

Shupti et al [4] performed 2D unsteady Newtonian & Non-Newtonian blood flow using the finite- volume method considering sinusoidally oscillating artery walls with time for the Reynolds numbers 300, 500 & 750.

Mamun et al [5] studied both non-Newtonian modelling effects on flows of fluid in physiology applying 3D idealized artery with single stenosis of 85% stenosis where the vessel wall is taken to be rigid & Reynolds number ranged from 96 to 800. Newtonian model has viscosity that is less than that of the non-Newtonian model when the shear rate ≤ 100 , but the viscosity of all models is equal when the shear rate is equal to or greater than 100 by Mamun et al [5].

* Corresponding author. Tel.: +88-01627285545

E-mail addresses: ahmadshayor963@gmail.com

: alfaruk.bd@gmail.com

Young et al. [6] studied pulsatile blood flow through the stenosis with an elastic wall to track the movement of the lumen. Their analysis found that shortly before the minimal lumen location, the greatest WSS was recorded. Ahmed et al. (1984) [7] case was that a rigid tube with constrictions of 25%, 50%, and 75% was tested for both steady and pulsatile flow with Reynolds numbers ranging from 500 to 2000. They used LDA to measure the pulsed flow field when symmetric stenosis was present. They tested using a sinusoidal velocity profile, 7.5 Womersley, 25, 50, and 75% area reduction stenoses, and 600 average Reynolds numbers.

According to Ghalichi [8], the low-Re k -turbulence model appears to provide more precise predictions than the traditional k - ϵ model. Using 50%, 75%, and 85% stenosed models, Ghalichi et al. (1998) studied transient and turbulent flow throughout a Reynolds number range of 500 to 2000. Their research showed that the laminar flow model overestimates the vortex length when the flow is transitional or turbulent [8]. There is evidence that arterial stenosis, one of the most chronic diseases in humans that causes cardiovascular dysfunction, develops and progresses as a result of stenotic flows in the cardiovascular system and vascular wall deformability. According to some researchers, both the initial development of stenosis and the regeneration of the stenosis, found from balloon angiography, are caused by damage to the inner coating of the artery, known as the intima [9] and [10] respectively. It is known that once a modest stenosis occurs, the ensuing flow disorder affects the progression of the condition and the deformability of the arteries as well as altering the regional blood rheology. [11] Besides, Shupti et al [12] studied non-Newtonian fluid flow behaviour using stenosis with highest area decrease of 60% numbering only one with a moving wall. The flow becomes asymmetric in the case of single stenosis as the Reynolds number rises, prompting more research into the relationship between stenosis and aneurysm [12].

Deshpande et al. (1980), used a Laser Doppler Anemometer (LDA) to study sustained turbulent flow through tube with 75% stenosis with Reynolds values ranging from 5000 to 15000 [13]. Harloff et al. (2013), used 4D imaging techniques to investigate velocity of flow within a stenosed artery [14].

Additionally, in recent years, certain researchers, such as Saleem et al. (2014), have made significant contributions to the area of blood flow modelling in stenosed arteries [15].

Razavi et al. (2011), conducted a comparison of other viscosity models as well as the Newtonian model [16]. They came to the conclusion that as the level of stenosis grows, the flow later on after the throat section gets more disrupted, and WSS formation at the stenosis throat more noticeable. Ellahi et al. (2014). In a stenosed artery, an analytical investigation of the unsteady and incompressible flow of micropolar non-Newtonian fluid was investigated. They discovered that when the stenosis height grows, so does the flow impedance [17].

In order to analyze the flow's hemodynamic properties and comprehend the hemodynamic differences between 2D

axisymmetric and 3D models in pulsatile blood flow, Karimi et al. (2013) developed a 3D model of an axisymmetric stenosis in the common carotid artery and displayed comparisons of simulation results with experimental data. They found a nonsymmetric flow in the post-stenosis zone that can only be visualized through 3D modeling due to the presence of large secondary flows, particularly at diastole [18].

In an artery with a stiff wall, Tu et al. (1996) conducted a finite element numerical simulation to evaluate steady and pulsatile blood flow for various constriction levels and Re values. [19]

Saad et al. (1983) stated that "We have planned to compare our numerical analysis with previously published numerical predictions obtained from the standard k - ω turbulence flow model and laminar flow modelling methods to validate this model" [20].

2. Theory

The conservation laws of momentum, mass in specific domains must be respected when simulating isothermal fluid flow via confined sections. The best turbulence model for a given application is determined by a number of parameters, including the flow under consideration, CPU time, and the level of precision necessary.

$$\frac{\partial \rho}{\partial t} + \frac{1}{r} \frac{\partial(r\rho u_r)}{\partial r} + \frac{1}{r} \frac{\partial(\rho u_\theta)}{\partial \theta} + \frac{\partial(\rho u_z)}{\partial z} = 0 \quad (1)$$

Since the problem is assumed to be steady-state & incompressible, so time-dependent parameters

$$\frac{\partial \rho}{\partial t} \text{ \& } \rho \text{ dropped from the equation we get,}$$

$$\frac{1}{r} \frac{\partial(r u_r)}{\partial r} + \frac{1}{r} \frac{\partial(u_\theta)}{\partial \theta} + \frac{\partial(u_z)}{\partial z} = 0 \quad (2)$$

The following two equations define conventional k - ω model by relating turbulent kinetic energy (k) specific dissipation rate (ω):

k and ω equations

$$\frac{\partial}{\partial t}(\rho k) + \frac{\partial}{\partial x_i}(\rho k u_i) = \frac{\partial}{\partial x_j} \left(\Gamma_k \frac{\partial k}{\partial x_j} \right) + G_k - Y_k + S_k \quad (3)$$

$$\frac{\partial}{\partial t}(\rho \omega) + \frac{\partial}{\partial x_i}(\rho \omega u_i) = \frac{\partial}{\partial x_j} \left(\Gamma_\omega \frac{\partial \omega}{\partial x_j} \right) + G_\omega - Y_\omega + S_\omega \quad (4)$$

The kinetic energy of turbulence caused by mean velocity gradients is represented by the symbol G_k . G_ω stands for the generation of ω . The effective diffusivity of k and is represented by Γ_k and Γ_ω respectively. The turbulence-induced dissipation of k and is represented by Y_k and Y_ω . User-defined source terms include S_k and S_ω . The influence on the overall structure of the flow field is controlled by a low Reynolds number correction factor, which is given as:

$$\alpha^* = \alpha_\infty^* \left(\frac{\alpha_0^* + Re_t/R_k}{1 + Re_t/R_k} \right) \quad (5)$$

Where $Re_t = \frac{\rho k}{\mu \omega}$, $R_k = 6$, $\alpha_0^* = \frac{\beta_1}{3}$, $\beta_1 = 0.072$, $\alpha_\infty^* = 1$. Closure Co-efficient for the Transitional k - ω Model are $R_k = 6$, $\beta_1 = \frac{\beta_1}{3}$, $\beta_1 = 0.09$, $\alpha_\infty^* = 1$, $\alpha_\infty = 0.52$, $R_\beta = 8$.

In cylindrical coordinates, (r, θ, z) the Navier-stokes equation of motion for an incompressible fluid of constant dynamic viscosity μ , and density ρ are:

$$\rho \left[\frac{Du_r}{Dt} - \frac{u_\theta^2}{r} \right] = -\frac{\partial p}{\partial r} + f_r + \mu \left[\nabla^2 u_r - \frac{u_r}{r^2} - \frac{2}{r^2} \frac{\partial u_\theta}{\partial \theta} \right] \quad (6)$$

$$\rho \left[\frac{Du_\theta}{Dt} + \frac{u_\theta u_r}{r} \right] = -\frac{1}{r} \frac{\partial p}{\partial \theta} + f_\theta + \mu \left[\nabla^2 u_\theta - \frac{u_\theta}{r^2} + \frac{2}{r^2} \frac{\partial u_r}{\partial \theta} \right] \quad (7)$$

$$\rho \frac{Du_z}{Dt} = -\frac{\partial p}{\partial z} + f_z + \mu \nabla^2 u_z \quad (8)$$

Where,

$$\frac{D}{Dt} = \frac{\partial}{\partial t} + u_r \frac{\partial}{\partial r} + \frac{u_\theta}{r} \frac{\partial}{\partial \theta} + u_z \frac{\partial}{\partial z} \quad (9)$$

$$\nabla^2 = \frac{\partial^2}{\partial r^2} + \frac{1}{r} \frac{\partial}{\partial r} + \frac{1}{r^2} \frac{\partial^2}{\partial \theta^2} + \frac{\partial^2}{\partial z^2} \quad (10)$$

For Non-Newtonian fluid, The model proposed by Pierre Carreau was Carreau model [20] was defined by-

$$\mu = \mu_\infty + (\mu_0 - \mu_\infty) [1 + (\gamma_c \dot{\gamma})^2]^{n-1/2} \quad (11)$$

3. Numerical Modelling

The Mathematical Modelling including the geometry creation, meshing, solution of the physical flow through computational methods are as follows.

3.1 Geometry

SOLIDWORKS 2019 software package was used to do this job. A 2D multiple stenosed model was developed by using the stenosed formation formula (Eqn. 3.11) in equation driven command

$$\frac{r(z)}{D} = 0.5 - A \left[1 + \cos \frac{\pi z}{D} \right] \quad (12)$$

Where $A = 0.073$ for 75% stenosis, $-D \leq z \leq D$ with $Z = 0$ at the throat of the stenosis), D is upstream diameter of artery (in the present work, 1 cm), and $r(z)$ is the varying radius that changes with axial distance along z . The stenosed percentage is defined as $[1 - (r/R)^2]$. The throat and upstream arterial radius, are represented by r and R respectively. The length of the pre stenosed region is 50 mm and the length of the post stenosed region is 150 mm. The total range of stenosed region is 20mm. Whole geometry was drawn in SOLIDWORKS 2019.

Two models with stenosis were investigated in this study. Model 1 has a constriction that reduces the lumen area by 75%. The stenosis in Model 2 is more severe, with area reduction of 86%. To ensure fully developed upstream flow, D is prior to the stenosis, where D is the unblocked arterial diameter. The outlet boundary condition was placed 20 diameters away from the throat to allow flow to redevelop.

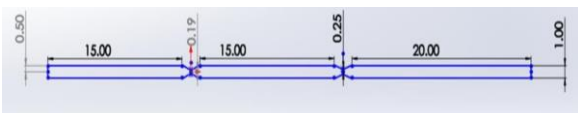


Fig.1 Geometry development of Multiple Stenosed Artery

3.2 Blood and Blood Vessel Properties:

In reality blood is a very complex fluid which is non-Newtonian, non-homogenous and incompressible. To make the analysis easier, the following assumptions were made:

- (i) The fluid (blood) is homogeneous, incompressible, and non-Newtonian, with a constant kinematic viscosity of $0.0035 \text{ m}^2/\text{sec}$ and mass density of 1060 kg/m^3 .
- (ii) The steady flow consideration is valid for large arteries with a more or less constant flow. There is a constant forward flow during diastole, which lasts around two-thirds of the heart cycle.
- (iii) Arterial walls are thought to be equally rigid.
- (iv) The stenoses employed in this investigation had a consistent form.

Table 1: Blood Properties

Density, μ (Kg/m ³)	1060
Steady Flow Velocity, v (ms-1)	0.315

3.3 Mesh

The meshing works were done in the ANSYS FLUENT software. After completing meshing procedures, a good grid is generated with 170471 nodes and 168000 elements. Six edges sizing was applied. It was noted that one biasing method was also applied

Edge sizing parameters are listed in **Table 2**.

After completing edge sizing, face meshing is applied for all faces. Mapped face meshing with quadrilateral type is applied. After executing these processes, a good structured C type mesh is generated with good mesh quality. Some good mesh quality figures are given below:



Fig.2: Meshing at Pre-Stenotic Region

Table 2: Characteristics of Edge Sizing

Parameters	Edge sizing 1	Edge sizing 2	Edge sizing 3	Edge sizing 4	Edge sizing 5	Edge sizing 6	Face Sizing
Geometry	2 edges	4 edges	4 edges	4 edges	4 edges	4 edges	Full Body
Type	Number of divisions	Number of divisions	Number of divisions	Number of divisions	Number of divisions	Number of divisions	
No of divisions	500	450	500	450	500	70	
Size function	Uniform	Uniform	Uniform	Uniform	Uniform	Uniform	
Behavior	Hard	Hard	Hard	Hard	Hard	Hard	
Biasing	No	No	No	No	No	Yes	
Bias option						Smooth transition	
Bias Factor						10	
Method							Quadrilaterals

Table 3: Quality of Edge Sizing

Quantity	Skewness	Orthogonal quality	Aspect Ratio
Maximum	0.66856	1	11.286
Average	4.6291e-002	0.99025	3.2504
Minimum	1.3057e-010	0.62904	1.0006
Standard deviation	7.6618e-002	2.0357e-002	2.218

Fig.3 shows the mesh for the 86% stenosed region. Here, at the artery wall inflation layers were incorporated to get fine mesh. Same was done for 75% stenosis.

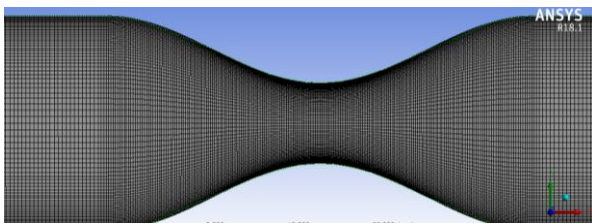


Fig.3: Meshing at 86% stenosis region

The mesh quality in multiple stenosed regions is shown in **Fig.4**. It can be seen that many black lines as there are huge amounts of nodes & elements here.



Fig.4: Meshing in the multi stenosis regions

3.4 Solver Settings

The governing equations were solved using a separate implicit scheme. The inlet was chosen as velocity inlet with constant average velocity. The outlet as pressure outlet (100 mmHg or 133322 kPa) The convective terms in momentum and turbulence equations were resolved using a second order upwind technique. The pressure term was attempted to be solved with a second-order scheme, and the pressure variable and velocity variable were coupled with SIMPLE method. The residual value was set to 10^{-6} because lowering the residuals was deemed unnecessarily due to use of higher-order discretization techniques. The number of iterations was given to 5000. Now in the workbench, the setup of static structure and FLUENT was coupled in the system coupling.

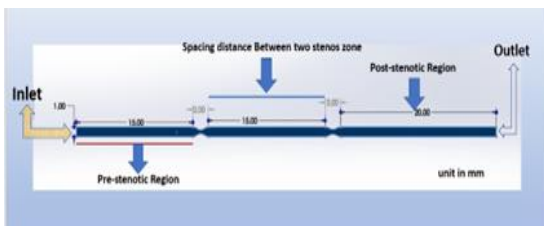


Fig 5: Boundaries of geometry of model blood vessel

4. Results and Discussion

Fig.6 shows the independency of results with mesh. Mesh independency test is done for mesh 0 (223,600 elements), mesh 1 (191,600 elements) & mesh 2 (160,160 elements) in multiple stenosed arteries. The characteristics pressure curve shows that, for mesh 1 & mesh 2, the pressure curve remains the same, while for mesh 0 condition it fluctuates. So, the generated grid is independent for mesh 1 & mesh 2.

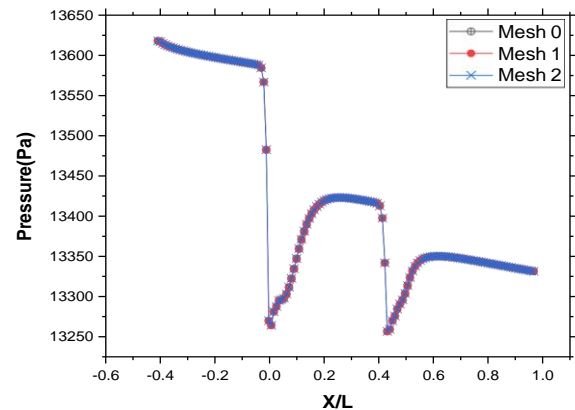


Fig.6: Grid Independence Test

The numerical results were compared to the laboratory findings published by Saad et al. [21] in terms of WSS at the constricted region in **Fig.7**. It's worth noting that they showed wall shear stress values at the stenotic throat, estimates based on velocity values taken at three stations at set distance from the wall. Results are likely depreciated values of the true wall shear stresses at the throat because the value of wall shear stress is highly responsive to the velocity profile near the wall. The forecasted wall shear stress at the throat is almost the same as the reported value of Galich et al. [8] according to the comparison.

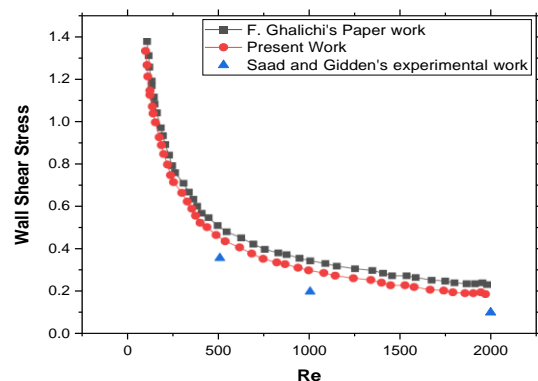


Fig.7: Validation Curve

The figures **Fig.8** and **Fig.9** shows the velocity and pressure fluctuation characteristic curves of single stenosis & multiple stenoses. In single stenosis, steep pressure drop happened in a single region while velocity increased. In multiple stenoses the pressure dropped in multiple regions gradually while velocity increased the same way as single stenosis but with more fluctuations.

In both cases at the throat regions velocity goes to the maximum level.

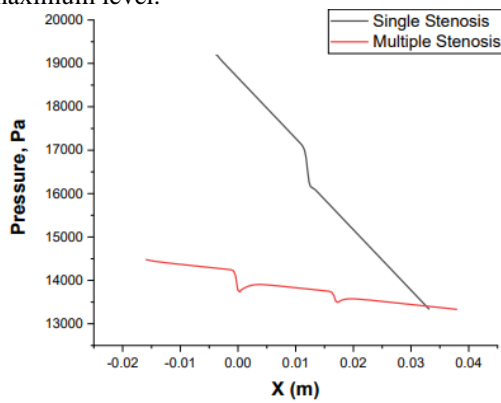


Fig.8: Pressure Difference between Single & Multiple Stenosis

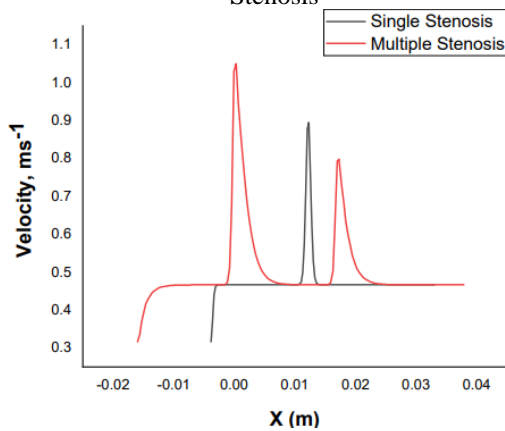


Fig.9: Velocity Difference between Single & Multiple Stenosis

Demonstrated in **Fig.10** the wall shear stress is gradually increasing in both models & in the throat regions, it goes to the maximum level. In the single stenosis region, the wall shear stress fluctuation is higher than in the multiple stenosis regions

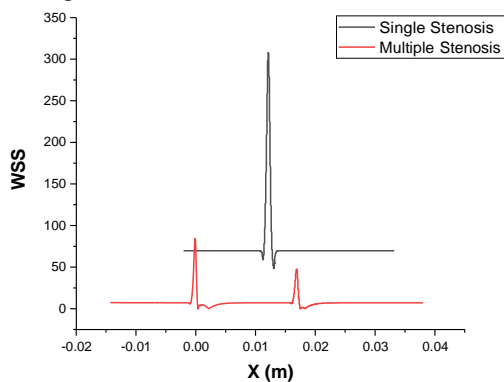


Fig.10: Wall Shear Stress Difference between Single & Multiple Stenosis

The turbulence intensity is gradually decreasing in multiple stenoses. On the other hand, in a single stenosis region, the turbulence intensity is decreasing instantly in **Fig.11**. In **Fig.12** the turbulence kinetic energy fluctuates,

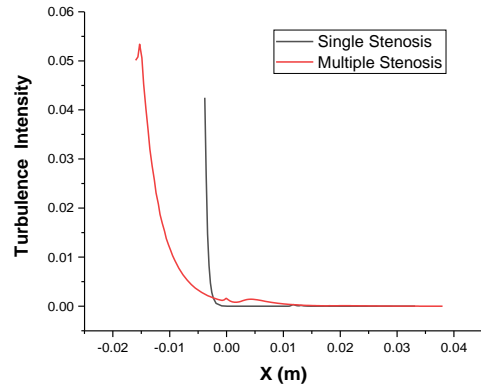


Fig.11: Turbulence Intensity Difference between Single & Multiple Stenosis

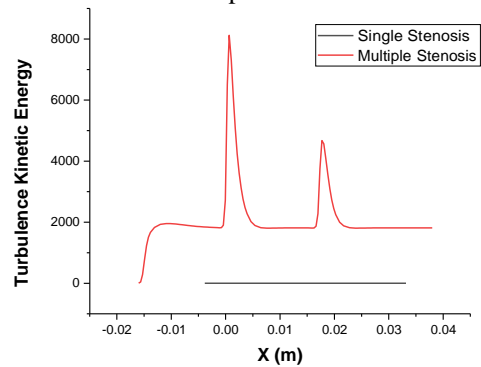


Fig.12: Turbulence Kinetic Energy Difference between Single & Multiple Stenosis

reaching peak value at stenosis. In a single stenosis region, the turbulence kinetic energy remains constant almost.

The fluctuations of pressure curves of multiple stenoses for different spacing distances between stenosis regions are shown in **Fig.13**. Pressure seems to be gradually decreasing in all the conditions dropping at multiple regions consisting fluctuations, the highest in the 86% stenosis region which is detrimental to health. **Fig.14** shows the velocity fluctuation curves of multiple stenoses for different spacing distances between stenosis regions. The rest of the curve behaves like **Fig.8**.

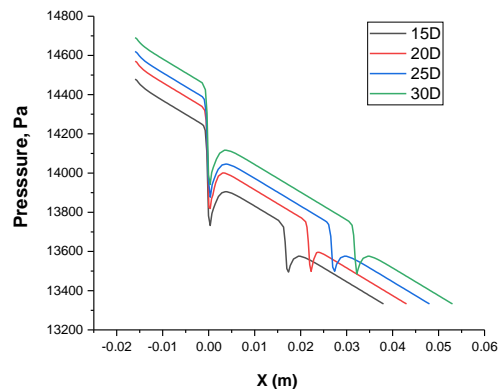


Fig.13 Pressure Charts for Different Spacing Distances

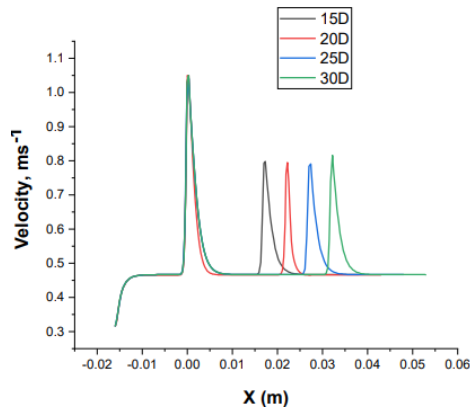


Fig.14 Velocity Chart for Different Spacing Distances

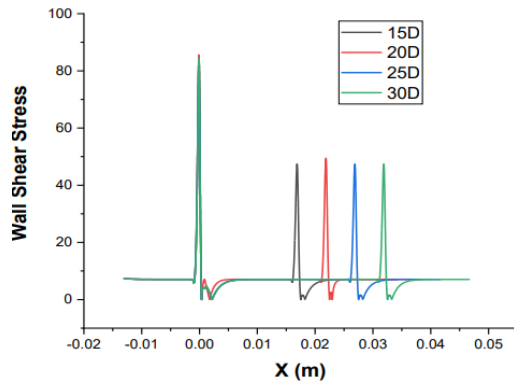


Fig.15: WSS Chart for Different Spacing Distances

Fig.15 shows wall shear stress characteristic curves of multiple stenoses for different spacing distances between stenosis regions can be seen. It can be concluded that the wall shear stress is gradually increasing in all the conditions & it goes to the maximum level in the 86% stenosis region.

Fig.16 results indicate that the turbulence intensity is gradually decreasing at 15D, 25D & 30D distances. On the other hand, at 25D distance, the turbulence intensity is increasing at the throat region. So, it can cause severe levels of heart problems

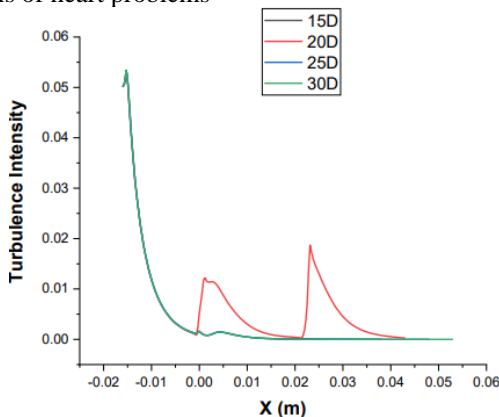


Figure 16 Turbulence Intensity Chart for Different Spacing Distances

Turbulence kinetic energy characteristic curves of multiple stenoses for different spacing distances show turbulence kinetic energy is gradually increasing in 15D, 20D & 25D conditions and in 30D conditions it remains constant by the depicted in **Fig.17**

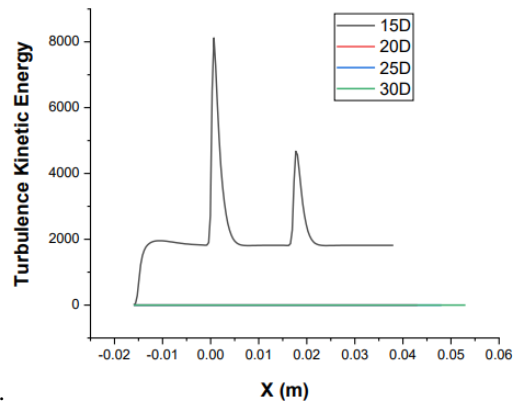


Fig.17 Turbulence Kinetic Energy Chart for Different Spacing Distances

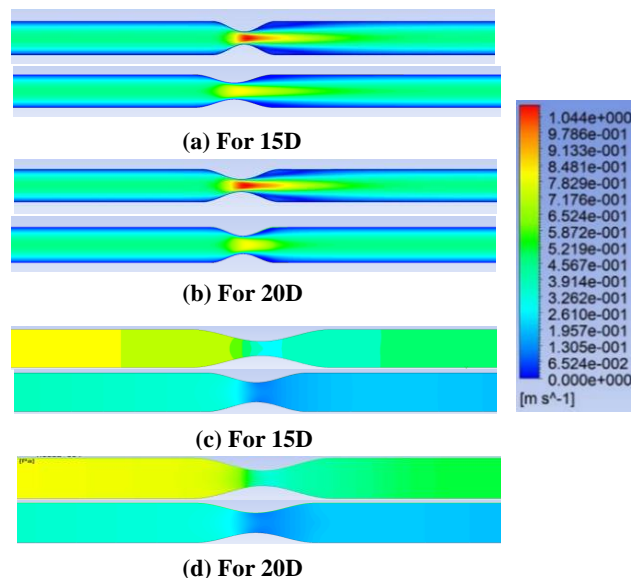


Fig.18 Contours (Pressure – (a), (b) and Velocity-(c), (d)) of 75% and 86% Stenosis Regions for 15D and 20D distances each

The velocity and pressure contours of multiple stenoses for 15D and 20D which show the main feature common for 25D and 30D comparison are shown in **Fig.18**. For 15D & 20D spacing distances, from the color bar, it can be seen that at pre-stenotic & post-stenotic regions, pressure remains at the upper mid-range value but at the stenotic region pressure drop is found and it falls down to the mid-range level. As in multiple stenosis regions, pressure is dropped in multiple regions, it can cause the instability of blood pressure & hamper the human natural comfort.

From the **Fig 20**, it can be seen that at the pre-stenotic region, stream function and vorticity contour remain constant & the flow characteristics are laminar. In the stenotic region, flow characteristics become transitional and in the post-stenotic region, they behave like a whirl formation which indicates that there is obviously a turbulence flow formed.

Before entering into the second stenosis which area constriction is 75%, the relaminarization is found in the pre-stenotic region of the above second figure.

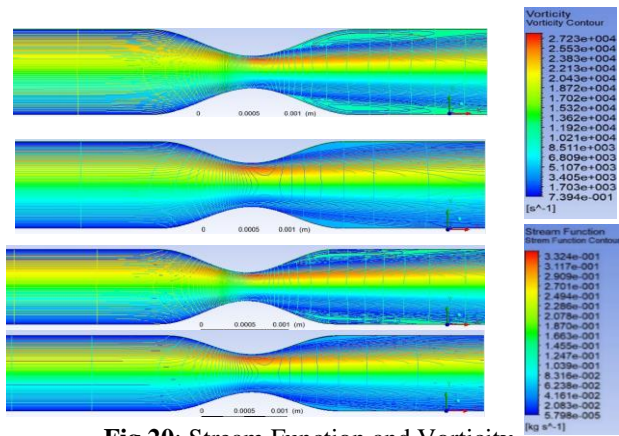


Fig 20: Stream Function and Vorticity Contour for 75% and 86% stenosis

Again, there is a turbulence formation of flow at the post-stenotic region of 75% stenosis. Thus, the laminarization & relaminarization happened in the stenoses regions.

From the shear stress curve, the primarily developed flow behaves more unstable in the stenosed region. In the stenosed region, shear stress increases & decreases more quickly, so there happened a transitional moment in the blood flow from laminar to turbulence. By following the above characteristics curves & their behaviors it can easily be concluded that in the stenosed region, blood flow characteristics behaved more unstable and more transitional. Thus, the fluid velocity changed with uncertainty as well as the pressure distribution.

These can cause the instability of blood pressure & hamper the human natural comfort. So multiple stenoses have higher impacts than single stenosis.

5. Conclusion

Key findings of this research work are listed below:

Velocity of the fluid increases in the stenosis region. Pressure dropping happens due to the constriction of the lumen area & the velocity increasing. Wall shear stress increases in the stenosis region. Turbulence kinetic energy increases with the increasing velocity. Turbulence intensity decreases in the stenosis regions.

Multiple stenoses have a higher impact on heart problems than single stenosis. Lower spacing distance has a higher level of discomfort scenario. In the pre-stenotic region fluid flow remains laminar. On the other hand, in the stenotic region flow characteristics remain transitional & in the post stenotic region, the fluid flow behaves laminar again. All these helps learn blood flow behavior in more detail contributing in developing better diagnostic device.

8. References

[1] Cardiovascular-diseases (CVDs), WHO international news room fact sheets
 [2] M. G. Rabby, A. Razzak, and Md. M. Molla, 5th BSME International Conference on Thermal Engineering, Dhaka (2012)
 [3] Tu, C., Deville, M., Dheur, L., and Vanderschuren L., "Finite Element Simulation of Pulsatile Flow Through Arterial Stenosis". *J. Biomech.* 25, 1141–1152 (1992)

[4] Sumaia Parveen Shupti, Md Mamun Molla and Mustak Mia, "Pulsatile Non-Newtonian Fluid Flows in a Model Aneurysm with Oscillating Wall", *Journal of Frontiers of Mechanical Engineering* (2017)
 [5] K. Mamun, M.N. Akhter, M.S.H. Mollah, M.A.N. Sheikh, and M. Ali, The 6th BSME International Conference on Thermal Engineering, Dhaka (2014)
 [6] V. Young, A. Patterson M. Graves, Z-Y LI, V. Tavani, T. Tang, and J. H. Gillard, *The British Journal of Radiology*, S39-S45 (2009)
 [7] S.A. Ahmed and D.P. Giddens, *Journal of Biomechanics*, 17, 695-705 (1984)
 [8] Farzan Ghalichi, Xiaoyan Deng, Alain De Champlain, Yvan Douville, Martin King and Robert Guidoin, "Low Reynolds Number Turbulence Modelling of Blood Flow in Arterial Stenoses" (1997)
 [9] R.M. Nerem, W.A. Seed, "An in Vivo Study of Aortic Flow Disturbances," *Cardiovas. Res.* 106,1-14(1972)
 [10] E. Speir, R. Modali, E.S. Huang, M.B. Leon, F. Shawl, T. Finkel, S. Epstine," Potential Role of Human Cytomegalovirus and P53 Interaction in Coronary Restenosis, *Science* 265, 391–394. (1994)
 [11] D. Liesch, "An Introduction to Biofluid Mechanics: Basic Models and Application", *Journal of Biomech.* 35, 415–435 (2002).
 [12] Rabby M. G., Sultana R., Shupti S. P., and Molla, M. M, "Laminar Blood Flow Through a Model of Arterial Stenosis with Oscillating Wall", *Int. J. Fluid Mech. Res.* 41, 417–429 (2014).
 [13] Deshpande, MD, Giddens DP. "Turbulence Measurements in A Constricted Tube", *J. Fluid Mech* 97:65–89 (1980)
 [14] Harloff A., Zech T., Wegent F., Strecker C., Weiller C., and Mark M., "Comparison of Blood Flow Velocity Quantification by 4D Flow MR Imaging with Ultrasound at The Carotid Bifurcation", *American Journal of Neuroradiol* 34, 1407–1413 (2013)
 [15] Saleem N., Hayat T., and Alsaedi A., "A Hydromagnetic Mathematical Model for Blood Flow of Carreau Fluid", *International Journal of Biomath* 7, 1450010 (2014)
 [16] Razavi A., Shirani E. and Sadeghi M. R., "Numerical Simulation of Blood: Pulsatile Flow in A Stenosed Carotid Artery Using Different Rheological Models", *J. Biomech.* 44, 2021–2030 (2011).
 [17] Ellahi R., Rahman S. U., Gulzar M. M., Nadeem S., and Vafai K., "A Mathematical Study of Non-Newtonian Micropolar Fluid in Arterial Blood Flow", (2014)
 [18] Karimi S., Dadvar M., Dabagh M., Jalali P., Modarress H. and Dabir B., "Simulation of Pulsatile Blood Flow Through Stenotic Artery Considering

- Different Blood Rheologies: Comparison of 3D and 2D-Axisymmetric Models”, *Biomedical Eng. Appl. Basis Commun.* 25, 1350023 (2013)
- [19] Tu, C., Deville and M., “Pulsatile Flow of Non-Newtonian Fluids Through Arterial Stenoses”, *Journal of Biomech* 29, 899–908 (1996)
- [20] Ahmed S. A., and Giddens D. P., “Velocity Measurements in Steady Flow Through Axisymmetric Stenoses at Moderate Reynolds Numbers”, *Journal of Biomech.* 16, 505–516 (1983).
- [21] P.J. Carreau, Transactions of The Society of Rheology, 16, 1957-1977 (1972)
- [22] Ali Ostadfar, Fluid Mechanics and Biofluids Principles, *Biofluid Mechanics, Principles and Applications*, pg. 26-27, 2016.

NOMENCLATURE

- c_p : specific heat at constant pressure, $\text{kJ} \cdot \text{kg}^{-1} \cdot \text{K}^{-1}$
- F : Helmholtz function, kJ
- G : Gibbs function, kJ
- h : specific enthalpy, $\text{kJ} \cdot \text{kg}^{-1}$
- p : pressure, kPa
- T : temperature, K
- t : Celsius temperature, $^{\circ}\text{C}$
- V : volume, m^3